A Geometric Framework for Mesoscale Models of Recrystallization

J.P. THOMAS, F. MONTHEILLET, and S.L. SEMIATIN

Geometric aspects are a major issue in models of recrystallization that rely on statistical grain-population descriptions, because the growth of recrystallized grains has to be compensated by the loss of volume of deformed grains, thus leading to concomitant variations in all geometric variables. A geometric framework for such models was thus designed. It is based on meso-structure units (MSUs), each of which represents an aggregate of similar grains. The evolution of MSUs is controlled by two kinds of inputs, nucleation rates and grain-boundary velocities, from which the evolution of microstructure is described in an internally consistent fashion. The geometric framework was applied initially to the necklace recrystallization of fine-grain microstructures, *viz*., the usual form of recrystallization comprising nucleation on initial grain boundaries. It was extended to describe particle-stimulated nucleation (PSN) in order to treat geometric effects related to intragranular recrystallization, as is found in coarse ingot micro-structures. For both the necklace-only and necklace-and-PSN cases, test cases using simple inputs were performed to validate the behavior of the geometric framework.

DOI: 10.1007/s11661-007-9247-x

I. INTRODUCTION

MODELING tools for the prediction of microstructure evolution are needed to optimize thermomechanical processes, *i.e*., to obtain desirable mechanical properties and to reduce both process design time and manufacturing cost. The usual method, based on the so-called Avrami or Johnson-Mehl-Avrami-Kolmogorov (JMAK) formulation, has been applied with some success for a number of years. In particular, its implementation in finite-element-method (FEM) subroutines, requiring minimal additional computational power, has provided a very useful tool for manufacturers.[1] However, such models become increasingly phenomenological as their domain of application is extended over wider ranges of temperature, strain, and strain rate, and for complex sequences of dynamic, metadynamic, and static recrystallization, as illustrated in Reference 2.

As long as dynamic recrystallization can be neglected or represented using reasonable approximations, it is possible to integrate a number of mechanisms and couple them inside the framework of an Avrami formulation.[3] However, the Avrami approach poses a number of limitations related to its lack of a true physical basis outside the context of classical static evolution. For example, it is incapable of properly incorporating the influence of precipitates on dynamic recrystallization,[4] and its extension to deal with partial waves of dynamic or metadynamic recrystallization is questionable.[5] Geometric and texture effects are also rarely included in such instances. A more fundamental weakness of this phenomenological approach, even when focusing on a specific alloy, relates to the extensive and, hence, expensive experimentation required to characterize microstructure evolution over the full range of temperature, strain rate, and history variables and, thus, to fit such models. Furthermore, it is usually not possible to extend Avrami relations derived for one material to another, even in the same alloy class, because the model parameters have limited physical meaning.

Models of microstructure evolution based on the Monte-Carlo[6] and cellular-automata[7,8] techniques also have their own advantages and limitations. They provide an enhanced representation of the physics of evolution. Nevertheless, they require substantial computational power, thus preventing their application at every node of an FEM mesh. In such cases, analysis is limited to a rather small number of tracking points.

To meet the needs of industry, a new type of recrystallization model is required. Such a model should combine the key advantages of the Avrami approach (*i.e*., reasonable computational requirements) and physics-based models (*i.e*., the formulation and input parameters should be as meaningful as possible). Computational requirements concern not only the coupling of the microstructure model with the FEM process model, but also various aspects of the optimization routine used to adjust model parameters in order to replicate the laboratory data that provide the basis of the material description. Because of the complexity of the thermomechanical processes at both the macroscales and microscales, computational restrictions preclude the

J.P. THOMAS, Visiting Scientist, Air Force Research Laboratory, AFRL/MLLMP, is with the Universal Technology Corporation, Dayton, OH 45432. F. MONTHEILLET, CNRS Senior Scientist, is with the Ecole Nationale Supérieure des Mines, Centre SMS, CNRS UMR 5146, 42023 Saint-Etienne Cedex 2, France. S.L. SEMIATIN, Senior Scientist, Materials Processing/Processing Science is with the Air Force Research Laboratory, Materials and Manufacturing Directorate, AFRL/MLLMP, Wright-Patterson Air Force Base, OH 45433. Contact e-mail: lee.semiatin@wpafb.af.mil

Manuscript submitted October 19, 2006.
Article published online July 25, 2007.

local description of microstructure evolution for every grain. Instead, a simplified grain-population description which is based on a statistical approach at the mesoscale appears to offer promise.

Geometric evolution is a central issue in mesoscale models of recrystallization because, first, the loss in volume of some grains through nucleation has to be compensated for by an increase in the volume of some other entity and, second, the growth of the recrystallized grains has to be compensated for by the loss in the volume of other (deformed) grains. The latter consideration includes the so-called impingement of recrystallized grains: in the context of dynamic recrystallization, the deformed grains may be not only the ones present at the very beginning of deformation; those of the previous generations of recrystallized grains may also be present. Hence, the impingement of the recrystallized grains during dynamic recrystallization rarely leads to the end of grain-boundary migration. As a result, the ability of mesoscale models to represent adequately the progress of recrystallized zones, the subsequent waves of the recrystallization that occur inside these zones, and, therefore, the dynamic steady state when recrystallization is complete depends primarily on the way in which geometric aspects are managed.

Given the complexity of the geometric issues, early mesoscale models neglected most of the evolution inside recrystallized zones during deformation.[9] Some improvements have been made, although the concept of impingement of grain boundaries stopping migration is typically assumed.[10,11] By contrast, the mesoscale model presented in Reference 12 focused on the steady state of dynamic recrystallization. In terms of geometry, the core of this model lay in the implicit evaluation of the probabilities of contact between grains of different types based on the surface of their boundaries. The same probability expressions were also used explicitly for the mesoscale modeling of static grain growth.[13] Inasmuch as this latter approach seems promising and applicable for a number of cases, it was thus chosen as the basis for the present work.

Mesoscale models should also reflect the distinction between the driving forces and mechanisms of microstructure evolution activated by deformation, on the one hand, and geometric evolution *per se* on the other. To deal with the strictly geometric effects of nucleation and grain growth discussed earlier, geometric variables should be constrained into a somewhat independent, yet internally consistent, framework that ensures that their coupled evolution satisfies volume conservation and that the geometric description of microstructures remains meaningful. In the present work, such a geometric framework for a statistical, mesoscale model for microstructure evolution is introduced. For purposes of statistical representation, grains of similar condition/state are aggregated into so-called mesostructure units (MSUs). Each MSU is defined by variables that can be seen as averages over the specific grain population which the MSU represents. Geometric variables include the volume density of the specific type of grains and the average dimensions or volume of the grains. A few other variables, such as the Taylor factor or the dislocation density, can be added to represent deformation-related properties and driving forces; the incorporation of these latter variables is briefly treated in Reference 5 and will be discussed more extensively in a companion publication.

The geometric framework was designed to respond to two types of inputs: nucleation rates and grain-boundary velocities. These inputs are provided by the other part of the model; *i.e.*, the one that is related to the microstructure-evolution mechanisms and driving forces, an example of which is summarized elsewhere.[5]

Inspired by previous models,[5,12] the present geometric framework was developed in the context of a larger program the objective of which is to develop and validate models of microstructural evolution during the primary processing of ingots of nickel-base superalloys such as Waspaloy.[14] In the sections that follow, the fundamental rules used to design the geometric framework are introduced first. The application of the framework for a strictly-necklace-recrystallization topology and its response for various simple input expressions are then described. Subsequently, the framework is extended to treat particle-stimulated nucleation (PSN) and the development of intragranular recrystallized areas. The challenges involved in quantifying the recrystallization behavior during ingot processing are discussed last.

II. FUNDAMENTAL ASPECTS OF THE GEOMETRIC FRAMEWORK

The definition and number of MSUs in the geometric framework depend on the specific use of the model. To represent a microstructure in which recrystallization occurs, at least two MSUs are required: one for the initial grains and one for the recrystallized grains (which consume the initial grains). However, additional MSUs may be beneficial in obtaining a more refined insight into microstructure evolution. For example, for multi-hit processes such as cogging, at least one other MSU is needed to distinguish between the recrystallized grains that appear during the current deformation step and those that appeared during previous bites, inasmuch as the latter grains are expected to be coarser and have higher dislocation densities than the ones developed during the current hit. In the present work, which aims at providing a general description of this geometric framework, the total number of MSUs is denoted as N_{MSU}. The N_{MSU} can be as low as 2 or 3, as discussed earlier, but it could be 50 or more as well, if the goal were to represent the distribution of strain hardening or grain sizes in the recrystallized structure with great accuracy. Large numbers of MSUs lead to computationally intensive models, however.

A. *Key Definitions*

Each MSU is designated by an index which varies from 1 to N_{MSU}; the numbering convention is that higher indices are assigned to the MSUs that contain more recent grains. Thus, MSU 1 comprises initial grains, while MSUs with higher indices are originally "empty"

(*i.e.*, contain no grains). The progressive filling and growth of MSUs of higher indices makes their volume, and thus the recrystallized fraction, increase.

In the isotropic case, the grains (for any MSU i) are assumed to be spheres of diameter D_i. Their volume density is denoted as n_i. The volume enclosed in the individual grain, v_{ei}, and the total volume of MSU i, V_i, are given by the relations

$$v_{ei} = \frac{\pi}{6} D_i^3 \qquad [1]$$

$$V_i = n_i v_{ei} = n_i \frac{\pi}{6} D_i^3 \qquad [2]$$

(In Eq. [1] and subsequent equations, the subscript e is used specifically for variables the definition of which relies on the surface enveloping each grain in the microstructure.)

The case of anisotropic grains is illustrated in Figures 1 and 2. It involves the definition of three dimensions, D_{xi}, D_{yi}, and D_{zi}, as the principal axes of the ellipsoid that provides the best-fit of the average grain of MSU i; v_{ei} and V_i are then given by

$$v_{ei} = \frac{\pi}{6} D_{xi} D_{yi} D_{zi} \qquad [3]$$

$$V_i = n_i v_{ei} = n_i \frac{\pi}{6} D_{xi} D_{yi} D_{zi} \qquad [4]$$

The total volume of the microstructure is the sum over i of all MSU volumes given by Eqs. [2] or [4]. The volume conservation issue appears clearly, as all geometric values are connected to this sum. Thus, the variation of any of them has to be compensated by the simultaneous change of some other(s). Practically, MSUs are initialized so that the total volume of the microstructure is equal to the unit volume. As a consequence, once volume conservation is assured during the entire course of microstructure evolution, the values V_i thus represent the volume fractions occupied by each MSU from which the recrystallized fraction(s) can be deduced in a straightforward manner.

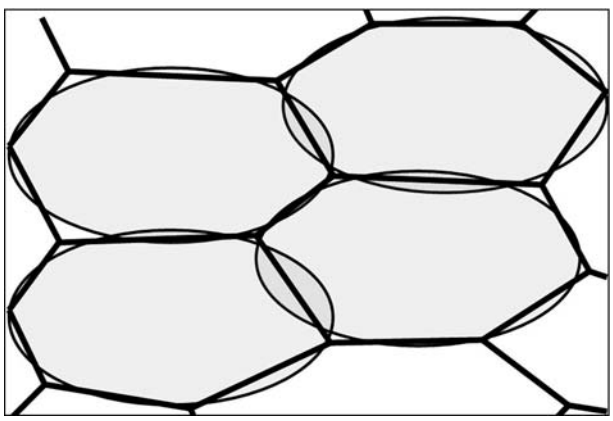

Fig. 1—Section of a schematic grain structure with the corresponding ellipsoidal-grain approximation.

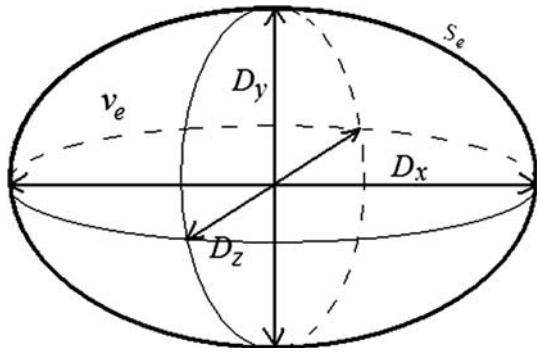

Fig. 2—Geometry of the ellipsoidal-grain approximation.

As a general and fundamental rule, the time rate of change of the volume of a grain, $\dot{v}$, is equal to the volume swept by its migrating grain boundary. Denoting the migration rate (which is normal to the grain boundary) as $\dot{u}$ and the boundary surface area as s, $\dot{v}$ is given by

$$\dot{v} = s\,\dot{u} \qquad [5]$$

Because the rate of variation of the grain dimensions is twice the average boundary velocity $\dot{u}_i$ of a grain of MSU i, Eq. [5] is readily verified for isotropic (spherical) grains. In this case, the surface area s_{ei} is given by

$$s_{ei} = \pi D_i^2 \qquad [6]$$

and the rate of variation of the volume enclosed by the grain boundary is

$$\dot{v}_{ei} = \pi D_i^2 \frac{\dot{D}_i}{2} = s_{ei} \dot{u}_i \qquad [7]$$

For anisotropic grains, the corresponding equation (which reduces to the proper expression in the limit of a spherical grain) is

$$\dot{v}_{ei} = \frac{\pi}{3} \left(D_{xi} D_{yi} + D_{yi} D_{zi} + D_{zi} D_{xi} \right) \dot{u}_i \qquad [8]$$

which leads to the following for the surface area in order to satisfy Eq. [5]:

$$s_{ei} = \frac{\pi}{3} \left(D_{xi} D_{yi} + D_{yi} D_{zi} + D_{zi} D_{xi} \right) \qquad [9]$$

Equation [9] is different from typical expressions for the surface area of an ellipsoid, which can be expressed analytically only for the specific cases of prolate and oblate spheroids. The reason for this discrepancy lies in the fact that when the surface of an ellipsoid migrates under the effect of a pressure, it does not remain ellipsoidal, contrary to the assumption underlying the derivation of Eq. [8] Compared to the exact solutions for oblate and prolate spheroids, however, Eq. [9] provides a result that differs by a maximum of ~30 pct for highly anisotropic shapes. In addition, it has the advantage of straightforward numerical evaluation applicable in all instances, even when all three principal axes are of different lengths in which case the surface area should be

evaluated using an elliptic integral. As a consequence, Eq. [9] provides a useful estimate for anisotropic grains the shapes of which approximate, but are not equivalent to, ellipsoids. Furthermore, this approximation is useful in addressing issues related to space filling, contact, and MSU interactions discussed later.

The density of the grain envelopes of MSU i in the whole structure, denoted S_{ei}, is defined as

$$S_{ei} = n_i s_{ei} \quad [10]$$

In Figure 3, this value for recrystallized grains, S_{e2}, is the sum of all grain envelopes represented in that section by thin lines. In zones such as the dashed square, the grain-boundary density inside MSU i only, S_{vei}, is defined by

$$S_{vei} = \frac{s_{ei}}{2\, v_{ei}} = \frac{1}{D_{xi}} + \frac{1}{D_{yi}} + \frac{1}{D_{zi}} \quad [11]$$

The factor of 1/2 in Eq. [11] is added to account for the fact that each grain boundary is the combination of two grain envelopes and thus avoids double-counting of the grain boundary between adjacent grains. As it is defined to describe zones for which the grains of only one MSU are represented, it is useful to evaluate interactions between grains of the same MSU.

B. *Principal and Secondary Variables*

Among the interrelated variables mentioned here, several are chosen to be the principal ones to describe the microstructure and to be those from which all others can be deduced. In this regard, volume conservation is a major concern, and model results are obtained *via* numerical integration using Runge–Kutta-type algorithms which involve linear combinations of derivatives

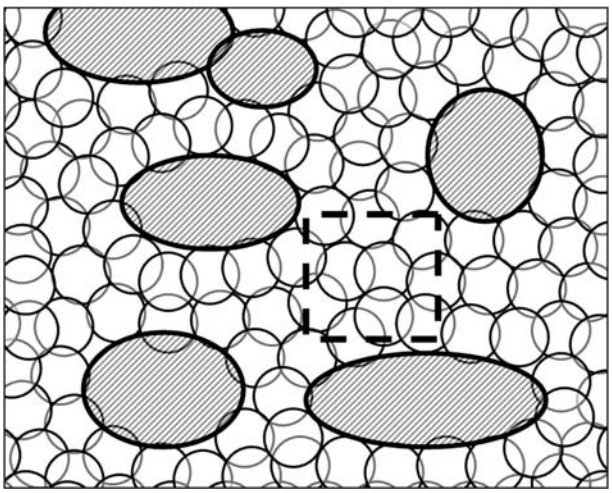

Fig. 3—Schematic cross section of a two-MSU microstructure. Initial grains (MSU 1) are cross-hatched, and their envelopes are thick lines. Recrystallized grains (MSU 2) are white and their envelopes are thin lines; surface areas s_{e1} and S_{e1} are represented by thick lines; s_{e2} and S_{e2} are represented by thin lines. The total envelope surface area S_{etotal} (= S_{e1} + S_{e2}) counts each grain boundary twice. In the dashed square, only interactions between grains of MSU 2 occur; they are treated using the grain-boundary density $S_{ve2} = 0.5\, s_{e2}/v_{e2}$.

evaluated at different steps. Hence, it is preferable that all derivatives be written in terms of volumes and not involve other variables such as grain size *per se*. By this means, the linear combination of a set of volume-conserving volumetric time rates of change results in a new set that is naturally volume conserving as well.

For the case of the necklace-only topology, MSUs are primarily defined by their volume V_i, the volume of their grains v_{ei}, and two anisotropy parameters α_{xyi} and α_{xzi}, only the derivatives of which have to be determined for subsequent integration. The parameters α_{xyi} and α_{xzi} are defined as the ratios of D_{yi} to D_{xi} and D_{zi} to D_{xi}, respectively. For each MSU i, these four principal variables are enough to deduce the secondary variables which include the density of grains n_i (Eq. [2]) and an additional intermediate, equivalent grain size D_{eqi}:

$$D_{eqi} = \left(\frac{6\, v_{ei}}{\pi}\right)^{1/3} \quad [12]$$

All three grain dimensions are derived from the equations

$$D_{xi} = \frac{D_{eqi}}{\left(\alpha_{xyi}\alpha_{xzi}\right)^{1/3}} \quad [13]$$

$$D_{yi} = D_{xi}\, \alpha_{xy\,i} \quad [14]$$

$$D_{zi} = D_{xi}\, \alpha_{xz\,i} \quad [15]$$

The surface quantities s_{ei}, S_{ei}, and S_{vei} are obtained from Eqs. [6], [9], [10], and [11].

For isotropic (spherical) grains, the anisotropy parameters α_{xy} and α_{xz} are equal to unity. Thus, D_i is equal to D_{eqi} and does not require further treatment during integration. For anisotropic grains, once the rate of variation of the volume enclosed within the grain is known, the variation rate of the grain dimensions can be obtained by rearranging Eq. [5] and applying the assumption that the variation rates for all three grain dimensions are the same, *i.e.*, twice the average grain-boundary velocity:

$$\dot{D}_i = \dot{D}_{xi} = \dot{D}_{yi} = \dot{D}_{zi} = 2\frac{\dot{v}_{ei}}{s_{ei}} \quad [16]$$

Then, the variation rates of the two anisotropy parameters can be derived as well; *i.e.*,

$$\dot{\alpha}_{xy\,i} = \frac{\dot{D}_{yi}}{D_{xi}} - \frac{D_{yi}}{D_{xi}}\frac{\dot{D}_{xi}}{D_{xi}} = \frac{\dot{D}_i}{D_{xi}}\left(1 - \alpha_{xy\,i}\right) \quad [17]$$

$$\dot{\alpha}_{xz\,i} = \frac{\dot{D}_{zi}}{D_{xi}} - \frac{D_{zi}}{D_{xi}}\frac{\dot{D}_{xi}}{D_{xi}} = \frac{\dot{D}_i}{D_{xi}}\left(1 - \alpha_{xz\,i}\right) \quad [18]$$

For the necklace-only topology, only the rates of variation of the volume of the MSUs and their grains, $\dot{V}_i$ and $\dot{v}_{ei}$, respectively, are thus necessary to calculate the geometric evolution of the whole microstructure.

III. GEOMETRIC FRAMEWORK FOR NECKLACE TECHNOLOGY

In this section, the dependence of $\dot{v}_{ei}$ and $\dot{V}_i$ on the grain-boundary velocities $\dot{u}_{ij}$ between grains of each pair i-j of MSUs and the nucleation rates $\dot{n}_i^{\text{nucl}}$ generated by each grain of MSU i are summarized. The nucleus volume, v^{nucl}, is assumed to be known and to be the same for all MSUs.

The geometric description for the volume variations due to the generation of nuclei is very simple, but becomes increasingly complex when quantifying volume variations related to the interactions between different MSUs, the interactions between grains of the same MSU, and the incorporation of nuclei into the MSU of highest index. The volume variations due to nuclei generation are given by

$$\dot{v}_{ei}^{\text{nucl}-} = \dot{n}_i^{\text{nucl}} v^{\text{nucl}} \quad [19]$$

$$\dot{V}_i^{\text{nucl}-} = n_i \dot{v}_{ei}^{\text{nucl}-} \quad [20]$$

The volume variations associated with the other phenomena are summarized in the following sections.

A. *Interactions between Grains of Different MSUs*

In order to calculate the interaction of the grains of MSU i with those in another MSU j, it is necessary to decompose the volume variation of their grains into the sum of the volume variations due to interactions with all MSUs:

$$\dot{v}_{ei}^{\text{migr}} = \sum_{j=1}^{N_{\text{MSU}}} \dot{v}_{ij}^{\text{migr}} = \sum_{j=1}^{N_{\text{MSU}}} s_{ij}\, \dot{u}_{ij} \quad [21]$$

Here, $\dot{v}_{ij}^{\text{migr}}$ is the volume variation of a grain i due to its interaction with grains of MSU j, s_{ij} represents the statistical probability of the surface of contact of a grain of MSU i with the grains of MSU j, and $\dot{u}_{ij}$ is the migration rate of a grain i–grain j boundary. Assuming a uniform probability of contact with grains of any MSU j among all the grains of the microstructure, s_{ij} is given by

$$s_{ij} = q_j s_{ei} \quad [22]$$

$$q_j = \frac{n_j s_{ej}}{\sum_{k=1}^{N_{\text{MSU}}} n_k s_{ek}} = \frac{S_{ej}}{S_{\text{total}}} \quad [23]$$

in which q_j is the probability that a grain-envelope surface element is in contact with the envelope of a grain of MSU j (and thus defines a grain boundary with that grain), when chosen randomly among all grain envelopes of the microstructure. The S_{total} is the total grain-envelope surface density present in the microstructure, *viz*., twice the total grain-boundary surface density (Figure 3). The probability q_j is thus a specific fraction of the envelope/boundary of a grain of MSU i. This choice is consistent with previous approaches.[5,12,13]

Figure 3 illustrates the simple case of a two-MSU microstructure. Because recrystallized grains (MSU 2) are fine and numerous, the probability/fraction $q_2 = S_{e2}/S_{\text{total}}$ has reached a value close to 1.0 as recrystallization progressed. In other words, the probability that a grain-envelope element is in contact with the grain envelope of a recrystallized grain is very high, and conversely, the probability of interaction with an initial grain is very low. Initial grains thus interact mostly with recrystallized grains but rarely with other initial grains, a behavior typical of a necklace topology.

The volume variation of a grain of MSU i due to its interaction with grains of MSU j is then given by

$$\dot{v}_{ij}^{\text{migr}} = s_{ij}\, \dot{u}_{ij} = s_{ei}\, q_j\, \dot{u}_{ij} = s_{ei} \frac{S_{ej}}{S_{\text{total}}}\, \dot{u}_{ij} \quad [24]$$

and the volume variation of the whole MSU i due to its interaction with MSU j is

$$\dot{V}_{ij}^{\text{migr}} = n_i s_{ij}\, \dot{u}_{ij} = n_i s_{ei}\, q_j\, \dot{u}_{ij} = S_{ei}\, q_j\, \dot{u}_{ij} \quad [25]$$

It can be readily shown that volume conservation is ensured; *i.e*.,

$$\dot{V}_{ij}^{\text{migr}} = n_i s_{ei} \frac{n_j s_{ej}}{S_{\text{total}}}\, \dot{u}_{ij} = -n_j s_{ji} \dot{u}_{ji} = -\dot{V}_{ji}^{\text{migr}} \quad [26]$$

B. *Interactions between Grains of the Same MSU*

Equations [24] and [25] are useful for interactions between grains of different MSUs. However, they are not applicable to the interaction among grains of their own MSU, because in-MSU interactions must leave the volume of the MSU unchanged while the migration of the boundaries that separate the grains of the MSU occurs. To deal with this case, analysis is focused on zones in which the grains of only one MSU are present, such as inside the necklace, for the case of a two-MSU microstructure (*e.g*., the dashed square of Figure 3). This case thus involves the use of the grain-boundary density S_{vei} defined by Eq. [11]). This relation is differentiated. Assuming an equal variation rate for each of the principal dimensions of the grains (as is assumed in Eq. [16]), the following is obtained:

$$\dot{S}_{vei} = -\dot{D}_i \left(\frac{1}{D_{xi}^2} + \frac{1}{D_{yi}^2} + \frac{1}{D_{zi}^2} \right) \quad [27]$$

Grain growth is related to the boundary density that disappears as a result of boundary migration. In other words, some moving boundaries meet each other, and only one boundary remains where there were two. However, at the scale of the whole microstructure, not all grain envelopes of MSU i are affected by this phenomenon, inasmuch as some are involved in interactions with grains of other MSUs. The contribution of in-MSU interactions is the balance after subtracting interactions with other MSUs, *i.e*., q_i. As a result, the volume swept by grain boundaries of MSU i, specifically

inside zones where only grains of MSU i are present, is given by

$$\dot{V}_i^{\text{swept}} = S_{vei}\, q_i\, \dot{u}_{ii} \quad [28]$$

Equation [28] is the equivalent for the in-MSU interactions of Eq. [25]. It gives the volume variation of MSU i related to the interactions between its own grains, which results actually in a null-volume variation, because it is taken over itself. Its only effect is to make the grain boundaries contained by this swept volume disappear:

$$\dot{S}_{vei}^{\text{migr}-} = S_{vei}\, \dot{V}_i^{\text{swept}} = \left(\frac{1}{D_{xi}} + \frac{1}{D_{yi}} + \frac{1}{D_{zi}}\right)^2 q_i\, \dot{u}_{ii} \quad [29]$$

Combining Eqs. [27] and [29], the contribution ($\dot{D}_{ii}^{\text{migr}}$) of boundary migration within an MSU to the grain-size variation of this MSU is obtained; *i.e.*,

$$\dot{D}_{ii}^{\text{migr}} = \frac{\left(1 + \frac{1}{\alpha_{xyi}} + \frac{1}{\alpha_{xzi}}\right)^2}{1 + \frac{1}{\alpha_{xyi}^2} + \frac{1}{\alpha_{xzi}^2}}\, q_i\, \dot{u}_{ii} \quad [30]$$

For isotropic grains, Eq. [30] becomes

$$\dot{D}_{ii}^{\text{migr}} = 3\, q_i\, \dot{u}_{ii} \quad [31]$$

In Eq. [31], the factor of 3 (instead of 2) may seem surprising. It is explained by the connection between grain-boundary velocity and the apparent grain-size variation of an MSU in which some grains grow and, most important, others disappear; *i.e.*, there is not a constant population. In such a case, MSU i is an aggregate of grains that would exhibit in reality a variety of sizes or stored energies. Depending on the purpose of the modeling, this could be an overly simplified representation. However, the geometric framework should not be modified depending on the context in which it is used. Hence, in practice, this approximation is either activated or prevented through the definition of the input of the framework. Specifically, the values for the velocity of the boundaries between the grains of a given MSU will be either zero or will assume some positive value (based on the dislocation density or grain-boundary curvature of MSU i and described by the driving force equations), if this feature is to be used. Lacking physical meaning, negative values are not possible.

From the rate of change of the grain size, the rate of change of the grain volume is readily derived as

$$\frac{\dot{v}_{ii}^{\text{migr}+}}{v_{ei}} = \frac{\dot{D}_{ii}^{\text{migr}}\, \left(D_{xi}D_{yi} + D_{yi}D_{zi} + D_{zi}D_{xi}\right)}{D_{xi}D_{yi}D_{zi}} = S_{vei}\, \dot{D}_{ii}^{\text{migr}} \quad [32]$$

C. *Incorporation of Nuclei by the MSU of Highest Index*

The incorporation of nuclei generated by the structure into the MSU of highest index (N_{MSU}) implies a volume increase of this MSU, and one can expect a refinement of its grain size. The rate of change of the volume of the MSU is the product of the total number of nuclei generated per unit time, $\dot{n}_{\text{total}}^{\text{nucl}}$, and the volume of the individual nucleus; *i.e.*,

$$\dot{V}_{N_{\text{MSU}}}^{\text{nucl}+} = \sum_{k=1}^{N_{\text{MSU}}} \dot{V}_i^{\text{nucl}-} = \dot{n}_{\text{total}}^{\text{nucl}}\, v^{\text{nucl}} \quad [33]$$

The differentiation of Eq. [2] for the case of the nuclei-receiver MSU (index N_{MSU}) yields

$$\dot{V}_{N_{\text{MSU}}}^{\text{nucl}+} = \dot{n}_{\text{total}}^{\text{nucl}}\, v_{e\,N_{\text{MSU}}} + n_{N_{\text{MSU}}}\, \dot{v}_{e\,N_{\text{MSU}}}^{\text{nucl}} \quad [34]$$

The combination of Eqs. [33] and [34] gives the rate of change of the volume of grains of the nuclei-receiver MSU as

$$\frac{\dot{v}_{e\,N_{\text{MSU}}}^{\text{nucl}}}{v_{e\,N_{\text{MSU}}}} = -\frac{\dot{n}_{\text{total}}^{\text{nucl}}}{n_{N_{\text{MSU}}}} \left(1 - \frac{v^{\text{nucl}}}{v_{e\,N_{\text{MSU}}}}\right) \quad [35]$$

As expected, the incorporation of nuclei induces a refinement of the grains of the MSU, inasmuch as the size of the nuclei is smaller than that of the grains of the MSU.

If the structure is completely recrystallized and, hence, all grains are in the MSU of highest index, interactions still occur and all nuclei are produced only within this MSU. The migration of the boundaries within the MSU produces a grain-size increase (Eq. [32]). Further nucleation tends to reduce its grain size (Eq. [35]). As a consequence, the geometric framework enables the model to function and reach a dynamic steady state even when only one MSU remains.

The simple addition or subtraction of the various rates of volume change enables the framework to incorporate inputs composed of nucleation rates and grain-boundary velocities into the volume variation rates of each MSU and of its grains, which can be readily integrated over time.

D. *Tests of the Framework Using Simple Input*

The geometric framework was encoded using C++. The core program comprised a generic MSU class the data sets of which consist of the primary geometric variables of MSUs. Various member functions were used to evaluate the secondary variables needed by the framework (grain dimensions, grain-boundary surfaces, *etc.*) The mesostructure was not implemented as a class but rather as a template that depends on a parameter class. It manages a flexible array of objects of its parameter class, which are expected to be MSUs when the template is instantiated. To calculate the geometric evolution in response to the inputs (the rates of nucleation and grain-boundary velocity), the mesostructure template relies on the values returned by the member functions of the objects of its array. These member functions have names and formats that are basically those of the generic geometric MSU class. This means that when it is instantiated, the mesostructure template must be built against a parameter class that

features at least the member functions of the generic geometric MSU class.

In practice, two steps are required to connect the geometric framework with mechanisms and driving forces to execute a complete mesoscale model. First, the generic geometric MSU is derived into a class that contains additional data sets (such as Taylor factor, dislocation density, *etc.*) and new member functions as needed. Second, the mesostructure template is instantiated against this new MSU class. This instantiation results in a mesostructure class in which all geometry evolution is managed transparently. Only the mechanisms of evolution, driving forces, and energy storage remain as the main focus for the model development and adjustment. For the simple tests presented in this article, the MSU derivation was concise, because only constant rates were used without explicit relation to any actual driving forces. However, for a mesoscale model applicable to an actual material, additional variables and a set of driving force equations, such as those briefly discussed in Reference 5, are needed.

The capabilities of the geometric framework for the necklace-only topology were evaluated using several hypothetical cases. These were based on constant rates of nucleation and grain-boundary migration varying by orders of magnitude. Although hypothetical in nature, the values used here were suggested by observations for Waspaloy within the temperature range of 1000 to 1120 °C and for strain rates between 0.01 and 1 s^{-1}.[4]

The first test of the framework was performed on a single MSU (which would apply if the microstructure were fully recrystallized) in order to evaluate the dynamic equilibrium provided by Eqs. [32] and [35]. A constant boundary velocity of 20 μm per unit strain and a nucleation rate of 1 nucleus per 10 μm^2 of grain boundary per unit strain were assumed for various initial grain sizes (Figure 4). The same steady-state grain size, indicative of a balance between nucleation and grain growth, was reached for all initial grain sizes tested.

A case comprising two MSUs was also analyzed to establish the influence of the competition between nucleation and grain-boundary migration on recrystallization. The first MSU was initialized with a 100-μm grain size. The second MSU, which incorporated the nuclei, was initially empty; its volume defined the recrystallized fraction of the structure. Various nucleation and migration rates were chosen to reach a recrystallized fraction of 50 pct at a deformation of approximately 0.5 for each of the chosen parameter combinations (Figure 5). The balance between nucleation and migration indirectly mirrors the influence of the strain rate on the recrystallization kinetics. At high strain rates, there is relatively little time for boundary migration and, thus, nucleation is responsible for most of the recrystallization. Conversely, most recrystallization at low strain rates occurs due to grain-boundary migration. An Avrami analysis of the obtained recrystallization kinetics revealed that an increase in the strain rate was accompanied by a decrease in the Avrami exponent (Figure 6).

The metadynamic evolution of recrystallization was tested by considering a zero nucleation rate after deformation and either a constant or a decreasing grain-boundary migration rate (Figure 7). The following expression quantified the influence of metadynamic recovery such as would give rise to a decreasing grain-boundary velocity:

$$\dot{u}_{\text{metadynamic}} = \dot{u}_{\text{dynamic}} \left(1 - \exp\left(\frac{t}{t_{\text{characteristic}}}\right)\right) \quad [36]$$

Very strong metadynamic recovery was found to inhibit the completion of recrystallization, as shown in Figure 7.

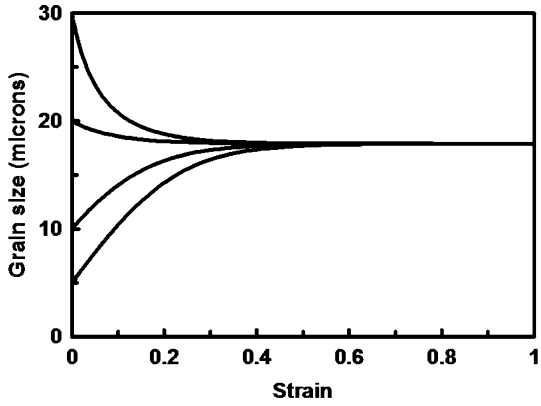

Fig. 4—Model results for the evolution of grain size during a single-MSU dynamic simulation. The nucleation rate was 1 nucleus per 10 μm^2 of grain boundary and per unit strain, the grain-boundary velocity was 20 μm per unit strain, and $v^{\text{nucl}} = 100\ \mu m^3$.

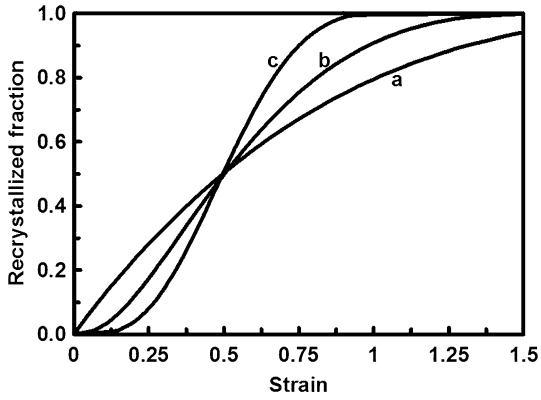

Fig. 5—Model results for recrystallized fraction during a two-MSU simulation of dynamic recrystallization. Nucleation rates were 1 nucleus per (*a*) 5 μm^2, (*b*) 100 μm^2, and (*c*) 5000 μm^2 of boundary and per unit strain; grain-boundary velocities were (*a*) 0 μm, (*b*) 42 μm, and (*c*) 105 μm per unit strain. $v^{\text{nucl}} = 100\ \mu m^3$.

IV. GEOMETRIC FRAMEWORK FOR NECKLACE-AND-INTRAGRANULAR TOPOLOGY

The approach presented in Section III is valid as long as the various grains only interact at their envelope surfaces. However, PSN of recrystallization within

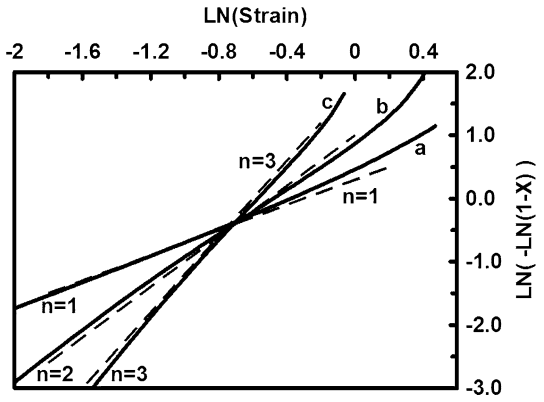

Fig. 6—Avrami analysis of the recrystallized-fraction curves in Fig. 5. X denotes the recrystallized fraction; the slope of the curves is the Avrami exponent n.

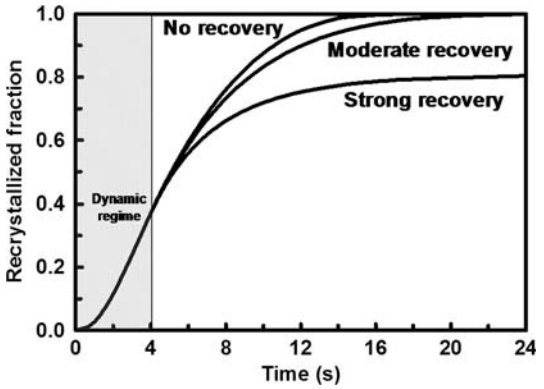

Fig. 7—Model predictions for the recrystallized fraction in two-MSU simulations of dynamic and metadynamic recrystallization. The nucleation rate was 1 nucleus per 100 μm^2 of grain boundary and per unit strain; the grain-boundary velocity was 42 μm per unit strain (equivalent to 4.2 μm/s to simulate a 0.1 s^{-1} strain rate during the dynamic regime). In Eq. [36], tested $t_{characteristic}$ values were 5 s (strong recovery), 20 s (moderate recovery), or an infinite time (no recovery). $v^{nucl} = 100\ \mu m^3$.

grains has been observed during the breakdown of coarse-grain superalloy ingot materials such as Waspaloy.[14] In such cases, the previous assumptions are not valid, inasmuch as the contact between grains of different MSUs does not lie solely along their envelopes. Rather, interfaces develop within the initial matrix due to the generation of recrystallized grains that nucleate (and subsequently) grow inside the initial grain(s), as illustrated in Figure 8. Therefore, the preceding equations have to be modified to account for a topology comprising both necklace and intragranular features.

Not all grains are subjected to intragranular nucleation. In practice, only relatively large initial grains exhibit such a topology. For fine initial grains, nucleation can also be enhanced by second-phase particles, but the intragranular recrystallized zones in these instances merge rapidly with the developing necklaces; as such, their intrinsic geometric influence can be neglected. Consequently, the intragranular topology is

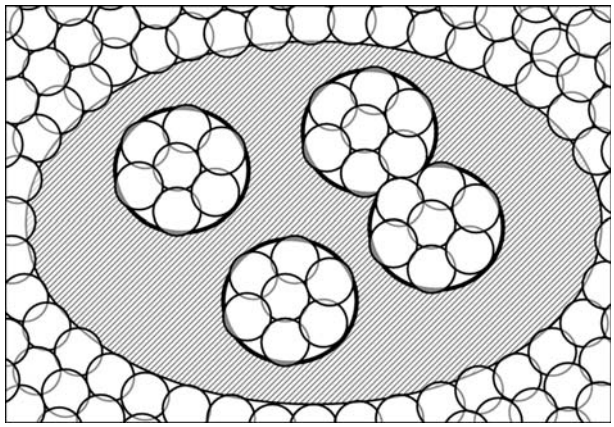

Fig. 8—Cross section of a two-MSU microstructure representing intragranular recrystallization within an ingot grain. The initial ingot grain (MSU 1) is cross-hatched, and recrystallized grains (MSU 2) are white. The thick lines delimit intragranular recrystallized zones, which would resemble bubbles in three dimensions; these thick lines are the location of a new kind of grain interaction not described by the equations for the necklace-only topology. s_{b1} and S_{b1} are thus represented by these thick lines; s_{e1}, S_{e1}, s_{e2}, and S_{e2} are represented by the thin lines.

only activated for the first N_{bt} MSUs of the structure when they are initialized for the case of coarse ingot grains. N_{bt} is strictly less than N_{MSU}. It means that the current recrystallized grains, stored in the MSU of highest index, do not represent sites for subsequent intragranular nucleation. In addition, in order to limit complexity, it is assumed that the only MSUs with grains that can fill the intragranular areas of others are those with indices that are greater than N_{bt}. In other words, intragranular recrystallized zones cannot be generated inside the intragranular zones of other MSUs through secondary PSN generation. This is not really a restriction, because the MSUs with an index strictly between N_{bt} and N_{MSU} will contain grains that recrystallized during the previous steps or hits of the simulated process. One can thus expect that they will not be coarse enough to develop the intragranular topology.

At the onset of PSN, intragranular zones contain only grains that nucleated on PSN particles. However, once recrystallized grains surround a particle, second and further generations of nuclei are generated in a manner formally similar to that of the necklace topology; *i.e.*, new nucleation sites for nuclei are provided at the new grain boundaries. Intragranular zones then spread out over the matrix, and, if the recrystallized grains they contain could be taken out, these zones would resemble growing bubbles. Therefore, the index "b" is used, in lieu of "e" for envelope, for variables that describe intragranular-related properties such as volume fraction, size, and surface area.

A. *Principal and Secondary Variables*

In order to take into account the intragranular zones, a new volume-related degree of freedom must first be defined. This volume has to allow space for the

development of intragranular zones. Thus, henceforth, v_{ei} in Eq. [3] represents the total volume enclosed within the grain envelope of MSU i, but not necessarily the volume of material that belongs to the grain itself. The latter quantity is denoted as v_i, and obviously it is less than or equal to v_{ei}. For instance, in Figure 8, the volume enclosed in the ingot grain envelope, v_{e1}, contains recrystallized zones. Thus, the volume of material that actually belongs to the ingot grain (denoted by the cross-hatching) is $v_1 < v_{e1}$. The difference between the two quantities is simply the recrystallized volume occupied by zones that develop around PSN particles. Therefore, v_i is the fifth principal variable needed for the geometric description of MSU i. It enables the description of intragranular recrystallized zones in a realistic and physically admissible way by defining an additional set of secondary variables, as summarized here.

First, the fraction X_{bi} of intragranular recrystallized zones contained by a grain of MSU i, and by extension in the whole MSU i, is defined as

$$X_{bi} = 1 - \frac{v_i}{v_{ei}} = 1 - \frac{V_i}{n_i\, v_{ei}} \qquad [37]$$

A new material parameter is needed for an accurate definition of the microstructure: the density of sites of volume nucleation, denoted n_{PSN}. Typically, n_{PSN} will be equal to the density of second-phase particles that induce a large enough local spread of crystallographic orientations to activate nucleation.[15] The average volume $v_{\mathrm{PSN}\ i}$ of a recrystallized zone that develops around a PSN site in the grains of MSU i can then be calculated. The volume of intragranular zones in a grain of MSU i is

$$\left(n_{\mathrm{PSN}} v_{ei}\right)\ v_{\mathrm{PSN}\,i} = v_{ei} - v_i \qquad [38]$$

Combining this relation with Eq. [37] leads to the desired relation

$$v_{\mathrm{PSN}\,i} = \frac{X_{bi}}{n_{\mathrm{PSN}}} \qquad [39]$$

Because the spatial distribution of particles may not be random, some clusters of PSN sites may behave as a single intragranular zone as $v_{\mathrm{PSN}\ i}$ increases. A new function $N_{\mathrm{cluster}}(v_{\mathrm{PSN}\ i})$, which quantifies the number of clustered particles depending on $v_{\mathrm{PSN}\ i}$, is then needed to evaluate the actual density of intragranular zones n_{bi} as $v_{PSN\ i}$ increases

$$n_{bi} = \frac{n_{\mathrm{PSN}}}{N_{\mathrm{cluster}}\left(v_{\mathrm{PSN}\,i}\right)} \qquad [40]$$

When $v_{\mathrm{PSN}\ i}$ is equal to zero, N_{cluster} assumes its minimum value of 1. In the case when no clustering occurs because the particles are randomly distributed, this function is also equal to unity.

The diameter D_{bi} of intragranular recrystallized zones that develop in the grains of MSU i is then given by

$$D_{bi} = \left(\frac{6X_{bi}}{\pi\ n_{bi}}\right)^{1/3} \qquad [41]$$

1. *Surface of interaction between the matrix of a grain and the intragranular recrystallized zones it contains*

In order to evaluate grain-interaction probabilities, the surface area between intragranular zones and the matrix of an initial grain must be calculated. If the assumption is made that intragranular zones are randomly distributed, the volume consumed by the growth of an intragranular zone is distributed between its surrounding matrix and its neighboring intragranular zones, with proportions equal to (on average) their respective volume fractions. In other words, due to the impingement between neighboring intragranular zones only a fraction 1-X_{bi} of the surface of intragranular zones is actually involved in interactions with the matrix of their initial grain. The surface area s_{bi} of interaction between the intragranular zones of a grain of MSU i and its matrix is then

$$s_{bi} = (1 - X_{bi})\ \left(v_{ei}\, n_{bi}\right)\ \pi\, D_{bi}^2 = v_i\, n_{bi}\, \pi\, D_{bi}^2 \qquad [42]$$

and the density of the surface of contact between the matrix and intragranular zones provided by the entire MSU i for the whole microstructure is

$$S_{bi} = n_i\, s_{bi} = V_i\, n_{bi}\ \pi\, D_{bi}^2 \qquad [43]$$

The interaction surface between intragranular zones and their surrounding grain makes it possible to investigate the various types of grain interactions and their respective contributions to recrystallization.

2. *Total grain-boundary densities*

As discussed with respect to Eq. [23], the calculation of the probability of contact of grains in one MSU (*i*) with those of another MSU (*j*) requires the evaluation of the fraction of the grain-interface density of MSU j relative to the total grain-interface density involved in these interactions. In the previous case of necklace-only topology, these grain interfaces were always the grain envelopes. However, when it comes to account for intragranular recrystallization, the situation is more complex, because two different types of grain interactions may occur.

The first and more common interaction is that investigated previously, *i.e.*, "envelope-envelope" interactions; the grain boundaries where such interaction takes place are defined by the contact of two grain envelopes.

The other interaction involves the contact of the envelope of a recrystallized grain with the initial grain along an intragranular interface (represented by thick lines in Figure 8 forming the so-called bubble referred to previously). By analogy with the previous envelope-envelope interactions, this other interaction is thus called a "bubble-envelope" interaction; the grain boundaries where such interactions take place are defined by the contact of a grain envelope with an intragranular bubble.

As a consequence, it is necessary to distinguish two total interaction surfaces denoted as $S_{e\ \mathrm{total}}$ and $S_{b\ \mathrm{total}}$, respectively. The latter is readily calculated as

$$S_{b\,\mathrm{total}} = \sum_{k=1}^{N_{bt}} n_k s_{bk} = \sum_{k=1}^{N_{bt}} S_{bk} \qquad [44]$$

The total surface density of grain boundaries involved in envelope-envelope interactions, $S_{e\mathrm{total}}$, is the total density of grain envelopes minus the part involved in bubble-envelope contact, which is $S_{b\ \mathrm{total}}$, because all bubbles are in contact with the envelopes of some recrystallized grains (the impingement of intragranular zones is already accounted for in Eq. [42]):

$$S_{e\,\mathrm{total}} = \sum_{k=1}^{N_{\mathrm{MSU}}} S_{ek} - S_{b\,\mathrm{total}} = S_{\mathrm{total}} - S_{b\,\mathrm{total}} \qquad [45]$$

Knowing these two total-boundary densities, it is possible to normalize grain-interaction probabilities.

3. *Partitioning of grain-interface areas between the two types of interaction*

A distinction is needed for individual grain-interface areas just as it was for total-boundary densities. For the grains of each MSU i, parameters q_{eei} and q_{bei} are defined as the fraction of their envelope in contact with the envelope of other grains or with the surrounding matrix, respectively, when they belong to an MSU some grains of which fill intragranular zones of low-index initial MSUs. For i less than or equal to N_{bt}, q_{bei} is zero inasmuch as these grains (initial grains) are not allowed to be in the intragranular recrystallized zones of other grains; in this case, q_{eei} is equal to 1. For other MSUs ($i > N_{bt}$), the assumption is made that each of them contributes to $S_{b\ \mathrm{total}}$ proportionally to its own surface:

$$S_{ebc\,\mathrm{total}} = \sum_{k=N_{bt}+1}^{N_{\mathrm{MSU}}} S_{ek} \qquad [46]$$

$$q_{bei}\ n_i s_{ei} = \frac{S_{ei}}{S_{ebc\,\mathrm{total}}} S_{b\,\mathrm{total}} \qquad [47]$$

Equation [47] involves an intermediate parameter, $S_{ebc\ \mathrm{total}}$, defined as the total density of the envelopes of the grains that can have nucleated in intragranular areas, and thus potentially contribute to $S_{b\ \mathrm{total}}$, *viz*., those with an MSU index strictly greater than N_{bt}. It can be simplified:

$$q_{bei} = \frac{S_{b\,\mathrm{total}}}{S_{ebc\,\mathrm{total}}} \qquad [48]$$

Furthermore,

$$q_{eei} = 1 - q_{bei} \qquad [49]$$

Equation [48] shows that all MSUs with envelopes that contribute to the surface of intragranular interfaces have the same partitioning between the two kinds of interactions.

4. *Interaction probabilities*

It is now possible to evaluate the probability of interaction for each pair of MSUs. The probability for a surface element of a grain boundary of MSU i to be an interface with a grain of MSU j (*i.e*., the relations corresponding to Eqs. [23] and [24] but for the case of a necklace-and-intragranular topology) is now described. Two new parameters, q_{eeij} and q_{beij}, are defined as the probabilities of contact involving envelope-envelope and bubble-envelope interactions, respectively.

The first probability, q_{eeij}, is the fraction of the envelope of a grain i that is in contact with the envelope of another grain (q_{eei}), multiplied by the fraction (q_{eej}) of the density of the grain envelopes of MSU j (S_{ej}) which is also in contact with a grain envelope, among all boundaries defined by an envelope–envelope contact ($S_{e\ \mathrm{total}}$):

$$q_{eeij} = q_{eei} \frac{q_{eej} S_{ej}}{S_{e\,\mathrm{total}}} \qquad [50]$$

Basically, the role of the product $q_{eei}\ q_{eej}$ in Eq. [50] is to restrict both the grain i and the MSU j to envelope-only aspects, resulting in the same fraction as the one given by Eq. [23], the expression for the probability of interaction for the envelope-only/necklace-only topology. Equation [50] is thus the generalization of Eq. [23] to the necklace-and-intragranular topology, and consistency is ensured because both q_{eei} and q_{eej} are equal to unity when there are no intragranular recrystallized zones. Conversely, when intragranular recrystallized zones develop, the behavior of the complementary parts $1–q_{eei}$ and $1–q_{eej}$, *viz*., q_{bei} and q_{bej}, must be taken into account.

The expression for q_{beij} depends on the value of i. If i is less than or equal to N_{bt}, then MSU i consists of ingot grains in which PSN can occur. Conversely, MSU j is composed of recrystallized grains, some of which are located in the intragranular zones of MSU i. Then q_{beij} is the fraction (q_{bej}) of the grain boundaries of MSU j (S_{ej}) in contact with intragranular interfaces (such as those of the grains of MSU i) relative to all interfaces between the intragranular recrystallized grains and the surrounding matrix ($S_{b\ \mathrm{total}}$):

$$q_{beij} = \frac{q_{bej} S_{ej}}{S_{b\,\mathrm{total}}} \qquad [51]$$

Conversely, if i is strictly greater than N_{bt}, MSU i is composed of recrystallized grains that can be inside the intragranular areas of MSU j. Then q_{beij} is the fraction (q_{bei}) of the grain envelopes of MSU i in contact with intragranular interfaces (such as those of the grains of MSU j), multiplied by the surface of intragranular interfaces present inside the grains of MSU j (S_{bj}), among all intragranular interfaces ($S_{b\ \mathrm{total}}$):

$$q_{beij} = q_{bei} \frac{S_{bj}}{S_{b\,\mathrm{total}}} \qquad [52]$$

Using these probabilities, it is possible to evaluate the time rates of change of MSUs and their grains in the various possible situations.

B. *Volume Variations of MSUs and Their Grains*

The rate of change of the volume of MSUs and of their grains depends on the interaction type, *i.e.*, both whether it is an envelope–envelope interaction or a bubble–envelope one and whether it is an interaction between grains of different MSUs or of the same MSU.

1. *Interactions between grains of different MSUs*

The interactions between different MSUs are the most numerous to deal with. The first, concerning interactions that involve only grain envelopes, affect v_{ei} and v_i with the same magnitude:

$$\dot{v}_{e\,ij}^{\text{migr}} = \dot{v}_{ij}^{\text{migr}} = q_{eeij}\, s_{ei}\, \dot{u}_{ij} \qquad [53]$$

$$\dot{V}_{ij}^{\text{migr}} = n_i \dot{v}_{ij}^{\text{migr}} \qquad [54]$$

The second, which are interactions between intragranular recrystallized grains and the ingot-grain matrix that surrounds them, consists of two symmetrical behaviors, depending on the location of grains. If we assume that i is less than or equal to N_{bt} and, conversely, that j is greater than N_{bt}, then the grains of MSU i contain some recrystallized j grains in their intragranular zones. For the former grains, there will only be a volume variation of the MSU and of its grains, but not of the volume delimited by their envelope because the latter is not involved:

$$\dot{v}_{e\,ij}^{\text{migr}} = 0 \qquad [55]$$

$$\dot{v}_{ij}^{\text{migr}} = q_{beij}\, s_{bi}\, \dot{u}_{ij} \qquad [56]$$

$$\dot{V}_{ij}^{\text{migr}} = n_i \dot{v}_{ij}^{\text{migr}} \qquad [57]$$

Conversely, for the j grains, all parameters will change, because their envelopes migrate through interaction with the intragranular interfaces of the first kind:

$$\dot{v}_{e\,ji}^{\text{migr}} = \dot{v}_{ji}^{\text{migr}} = q_{beji}\, s_{ej}\, \dot{u}_{ji} \qquad [58]$$

$$\dot{V}_{ji}^{\text{migr}} = n_j \dot{v}_{ji}^{\text{migr}} \qquad [59]$$

An examination of Eqs. [57] and [59] shows that all interactions conserve volume as required, despite the more complex scheme.

2. *Interactions between grains of the same MSU*

Interactions between grains of the same MSU involve envelope–envelope interactions only. They produce no change in the total volume of the MSU, but generate an increase in the volume and size of grains. Hence, the equations are similar to those obtained for the necklace-only topology. The intermediate rate of change of the grain dimensions is almost unchanged:

$$\dot{D}_{ii}^{\text{migr}} = \frac{\left(1 + \frac{1}{\alpha_{xy\,i}} + \frac{1}{\alpha_{xz\,i}}\right)^2}{1 + \frac{1}{\alpha_{xy\,i}^2} + \frac{1}{\alpha_{xz\,i}^2}}\, q_{eeii}\, \dot{u}_{ii} \qquad [60]$$

Converted to the corresponding volume variations, the following expressions are obtained:

$$\frac{\dot{v}_{e\,ii}^{\text{migr}+}}{v_{ei}} = S_{vei}\, \dot{D}_{ii}^{\text{migr}} \qquad [61]$$

$$\dot{v}_{ii}^{\text{migr}+} = (1 - X_{bi})\, \dot{v}_{e\,ii}^{\text{migr}+} \qquad [62]$$

3. *Effects of nucleation*

Two different nucleation rates are needed, depending on the location of the nucleation sites. Such sites can lie at (1) the periphery of grains, in which case the volume enclosed in their envelope is affected, or (2) the interfaces of intragranular recrystallized zones of ingot grains (initiated through PSN), which do not affect their envelope. The notations for the nucleation rates at the periphery of grains and at the interfaces of intragranular recrystallized zones are $\dot{n}_{ei}^{\text{nucl}}$ and $\dot{n}_{bi}^{\text{nucl}}$, respectively. Their sum is $\dot{n}_i^{\text{nucl}}$. The nucleus volume v^{nucl} is unchanged. The rates of change of the volume of MSU i and its grains due to the generation of nuclei are

$$\dot{v}_{ei}^{\text{nucl}-} = \dot{n}_{ei}^{\text{nucl}}\, v^{\text{nucl}} \qquad [63]$$

$$\dot{v}_i^{\text{nucl}-} = \left(\dot{n}_{ei}^{\text{nucl}} + \dot{n}_{bi}^{\text{nucl}}\right)\, v^{\text{nucl}} = \dot{n}_i^{\text{nucl}}\, v^{\text{nucl}} \qquad [64]$$

$$\dot{V}_i^{\text{nucl}-} = n_i \dot{v}_i^{\text{nucl}-} \qquad [65]$$

Expressions for the incorporation of generated nuclei by the MSU of the highest index obtained in Section III for the necklace-only topology are still applicable because this MSU does not allow PSN. The only modification is that the total nucleation rate $\dot{n}_{\text{total}}^{\text{nucl}}$ designates the sum for all MSUs of their two nucleation rates, *i.e.*, not only peripheral, but also intragranular:

$$\dot{V}_{N_{\text{MSU}}}^{\text{nucl}+} = \sum_{k=1}^{N_{\text{MSU}}} \dot{V}_i^{\text{nucl}-} = \dot{n}_{\text{total}}^{\text{nucl}}\, v^{\text{nucl}} \qquad [66]$$

$$\frac{\dot{v}_{e\,N_{\text{MSU}}}^{\text{nucl}}}{v_{e\,N_{\text{MSU}}}} = \frac{\dot{v}_{N_{\text{MSU}}}^{\text{nucl}}}{v_{N_{\text{MSU}}}} = -\,\frac{\dot{n}_{\text{total}}^{\text{nucl}}}{n_{N_{\text{MSU}}}} \left(1 - \frac{v^{\text{nucl}}}{v_{e\,N_{\text{MSU}}}}\right) \qquad [67]$$

Here again, the framework provides a tendency to reach a steady state when only the MSU that receives nuclei remains through an equilibrium between Eqs. [61] and [67].

C. *Evolution of Topologies*

One of the objectives of mesoscale models of recrystallization is the prediction of so-called ALA (as large as) grains, some of which may be remnants of the initial ingot grains. When such remnants persist, they may appear to be isolated due to the percolation of intragranular areas, resulting in continuous networks of recrystallized grains. These remnants may resemble the unrecrystallized initial grains of wrought microstructures, except for the fact that adjacent ALA grains may exhibit similar crystallographic orientations. Thus, partially wrought ingot microstructures may be better represented by a necklace-only topology once intragranular areas have reached a substantial fraction. This approach may be especially useful for quantifying the subsequent evolution of the isolated remnants of the coarse initial ingot grains.

To convert from one topological description to the other, the envelope density of isolated remnants, S_{ei}^{new}, is set equal to the sum of the preconversion envelope and the density of intragranular interfaces in order that the interaction surfaces remain identical:

$$S_{ei}^{\text{new}} = S_{ei} + S_{bi} = S_{bi}\left(1 + \frac{S_{ei}}{S_{bi}}\right) \quad [68]$$

Equation [68] ensures that all mechanisms that depend on grain-boundary densities (grain growth, nucleation, *etc.*) are continuous. As a consequence, not only are the recrystallized fraction and grain size continuous, but their slope before and after the conversion is the same. Considering that each isolated remnant is surrounded by N_{surround} intragranular recrystallized zones, each of which separates two remnants, the expression for the new grain density can be obtained:

$$n_i^{\text{new}}\,\frac{N_{\text{surround}}}{2} = n_{bi}\,(n_i v_{ei}) \quad [69]$$

$$n_i^{\text{new}} = \frac{2\,n_{bi}\,n_i\,v_{ei}}{N_{\text{surround}}} \quad [70]$$

The average diameter of these isolated remnants, D_i^{new}, can then be evaluated by equating the volume of MSU i before and after conversion and incorporating the result into Eq. [70]:

$$n_i^{\text{new}}\,\frac{\pi}{6}\,D_i^{\text{new}\,3} = n_i\,v_i = n_i\,v_{ei}(1 - X_{bi}) \quad [71]$$

$$D_i^{\text{new}} = \left(\frac{3\,N_{\text{surround}}}{\pi\,n_{bi}}(1 - X_{bi})\right)^{1/3} \quad [72]$$

The condition of surface density equality before and after conversion expressed in Eq. [68] can be expanded as

$$n_i^{\text{new}}\,\pi\,D_i^{\text{new}\,2} = n_{bi}\,(n_i\,v_{ei}\,(1 - X_{bi}))\,\pi\,D_{bi}^2\left(1 + \frac{S_{ei}}{S_{bi}}\right) \quad [73]$$

When combined with Eqs. [70], [72], and [41], this condition becomes

$$f(X_{bi}) \equiv N_{\text{surround}}\left(1 + \frac{S_{ei}}{S_{bi}}\right)^3 X_{bi}^2\,(1 - X_{bi}) = 2 \quad [74]$$

If the function f reaches a value of 2, it is possible to convert the initial ingot grains interspersed with intragranular grains into an equivalent set of necklace-only wrought-like grains. This function attains its maximum value when the fraction of intragranular zones reaches 2/3. The condition expressed in Eq. [74] then becomes

$$N_{\text{surround}}\left(1 + \frac{s_{ei}}{s_{bi}}\right)^3 = \frac{27}{2} \quad [75]$$

When the surface area of initial boundaries is negligible compared to that of the intragranular areas, the latter equation gives $N \sim 13.5$, a number that lies in the range of the number of faces of typical space-filling polyhedra that resemble grains, *e.g.*, the dodecahedron (12 faces) or tetrakaidecahedron (14 faces). The topological conversion is straightforward inasmuch as the volume of the whole MSU remains unchanged:

$$V_i^{\text{new}} = n_i^{\text{new}} v_{ei}^{\text{new}} = V_i = n_i\,v_i \quad [76]$$

$$v_{ei}^{\text{new}} = \frac{n_i}{n_i^{\text{new}}}\,v_{ei}(1 - X_{bi}) = \frac{N_{\text{surround}}}{2\,n_{bi}\,n_i\,v_{ei}}\,n_i\,v_{ei}\left(1 - \frac{2}{3}\right) = \frac{N_{\text{surround}}}{6\,n_{bi}} \quad [77]$$

Including the clustering effect (Eq. [40]), the following relation is obtained:

$$v_{ei}^{\text{new}} = \frac{N_{\text{surround}}}{6\,n_{bi}} = \frac{N_{\text{surround}}}{6}\,\frac{N_{\text{cluster}}(v_{\text{PSN}i})}{n_{\text{PSN}}} \quad [78]$$

Equation [78] indicates that the spatial distribution/clustering of PSN sites has a dramatic influence on the size of the remnants of initial grains, as might be expected. To improve the precision of the estimate, multiple levels of clustering could be defined instead of only one in order to represent the spatial ordering of PSN sites that may occur at different scales.

D. *Tests of the Geometric Framework Using Simple Input*

The behavior of the complete geometric framework for the necklace-and-intragranular topology was evaluated using several hypothetical cases in which constant rates of nucleation and grain-boundary migration were chosen based on the order of magnitude of those observed in practice for Waspaloy ingots.[14] The framework was tested using a two-MSU microstructure initialized with coarse anisotropic ingot grains measuring $2300 \times 2300 \times 23{,}000$ μm, *i.e.*, a volume equivalent to that of a 5000-μm sphere but with an aspect ratio of 10. A constant boundary velocity of 10 μm per unit strain and a nucleation rate of 1 nucleus per 100 μm^2 of grain-boundary per unit strain were assumed. The

density of PSN sites was taken to be 0, 1, 10, 100, and 1000 per mm^3. An acceleration of recrystallization induced by an increase in the density of PSN sites was clearly observed (Figure 9). It was accompanied by an increase in the Avrami exponent (Figure 10). Both results are well supported by experimental data[14] as well as by other modeling methods.[16]

Last, the full geometric framework was applied to describe the recrystallization of an ingot microstructure assuming 1000 PSN sites per mm^3. First, the behavior observed for randomly dispersed PSN particles was compared to that obtained with groups of ten particles clustered in spheres of approximately 200 μm. Model results revealed that clustering reduces the enhanced recrystallization effect of PSN (Figure 11). A modeling approach based on converting initial ingot grains to a wrought-like microstructure when the fraction of intragranular zones reached 2/3 was also tested; the subsequent evolution of the recrystallized fraction was almost identical to that without conversion (Figure 11). Furthermore, the beneficial effect of such an approach was made clear in a comparison of the size of the remnants of the initial grains (Figure 12). For the case in which the initial ingot grains are retained in the model until full recrystallization is achieved, the evolution of their size (defined by their envelope) is of little interest, especially during the final stage before they are totally consumed, because most of their recrystallization is actually intragranular. In the corresponding curve of remnant size *vs* strain (Figure 12), the initial ingot grains thus seemed to disappear suddenly. Hence, this approach in general fails to provide significant information about the zones in which evolution occurs. On the other hand, valuable information about the size of the remnants of the initial grains is obtained from the modeling approach involving the topological conversion. At the moment when the initial ingot grains were converted into wrought-like grains, the curve describing the size of the remnants exhibited a sudden change because the information it provided was no longer based on the initial envelope of the ingot grains (Figure 12); it then related to the volume enclosed in the envelopes of the new wrought-like grains. Due to Eq. [68], the envelopes of these grains are mostly inherited from the interfaces of the percolating intragranular zones in which most of the evolution occurs. They are the true remnants of initial grains that are to be dealt with as single entities instead of as a group enclosed in the initial envelope. As a result, the curve that follows the conversion provides the needed information. For the present example, it exhibited a smooth decrease until recrystallization was complete.

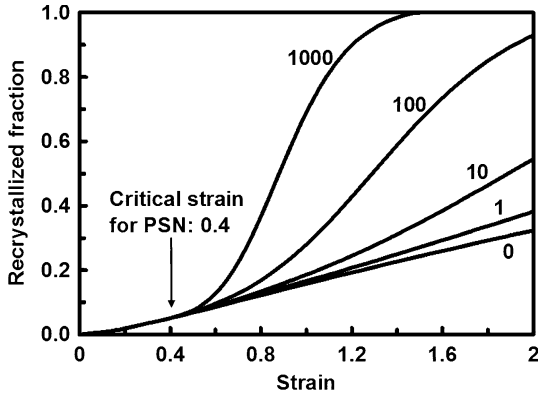

Fig. 9—Model results for the recrystallized fraction during the two-MSU simulation of the dynamic recrystallization of coarse ingot grains for various PSN-site densities per mm^3. The nucleation rate was 1 nucleus per 100 μm^2 of boundary and per unit strain, the grain-boundary velocity was 10 μm per unit strain, and v^{nucl} = 1000 μm^3.

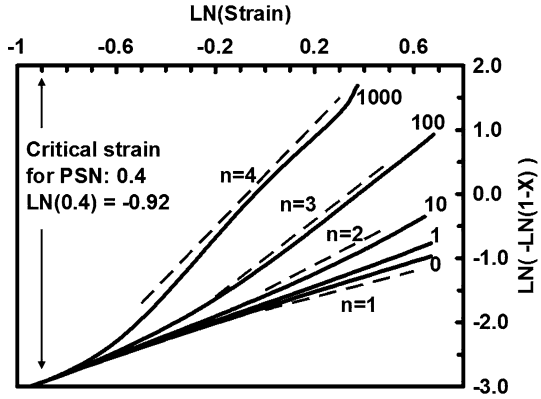

Fig. 10—Avrami analysis of the recrystallized-fraction curves in Fig. 9. *X* denotes the recrystallized fraction; the slope of the curves is the Avrami exponent *n*.

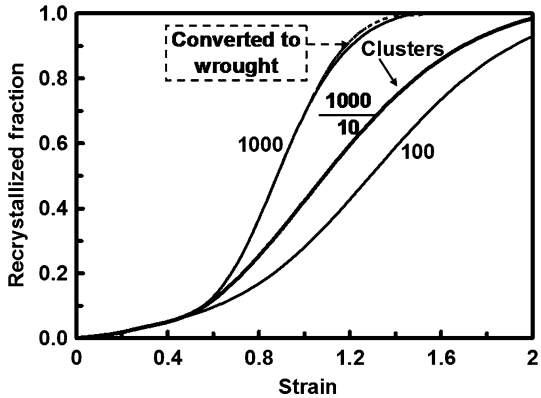

Fig. 11—Model results for the recrystallized fraction during two-MSU simulations of dynamic recrystallization assuming 100 or 1000 PSN sites per mm^3. For the 1000 PSN-site-density case, clustering of groups of 10 PSN particles in 200-μm spheres was evaluated, and conversion of initial ingot grains into wrought-like microstructures at an intragranular recrystallized fraction of 2/3 was performed. The nucleation rate was 1 nucleus per 100 μm^2 of boundary and per unit strain, the grain-boundary velocity was 10 μm per unit strain, and v^{nucl} = 1000 μm^3.

V. SUMMARY AND CONCLUSIONS

The geometric framework needed as a prerequisite for the development of a mesoscale-mechanism-based model of recrystallization was formulated. It can represent the geometric evolution of a wide variety of microstructures ranging from columnar-grain ingot materials with PSN to wrought alloys and responds to two kinds of

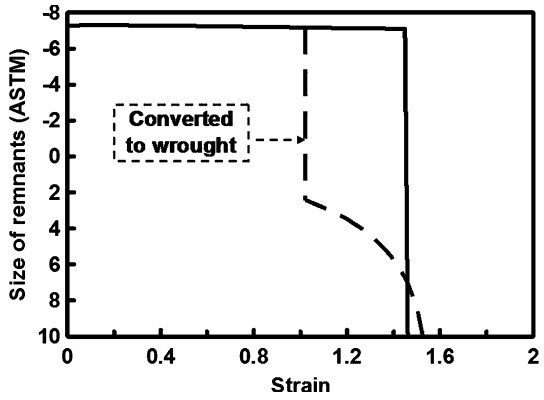

Fig. 12—Model results for the size of the remnants of initial ingot grains developed during two-MSU simulations of dynamic recrystallization, assuming 1000 PSN sites per mm^3. In the first case, ingot grains were kept until full recrystallization using intragranular topology, and in the second case (dashed line) initial ingot grains were converted into wrought-like grains when the fraction of intragranular zones reached 2/3 to allow the prediction of ALAs. The nucleation rate was 1 nucleus per 100 μm^2 of boundary and per unit strain, the grain-boundary velocity was 10 μm per unit strain, and $v^{nucl} = 1000\ \mu m^3$.

inputs: nucleation rates and grain-boundary velocities. Based on grain aggregates of similar properties or histories referred to as MSUs, the framework offers the flexibility to adapt the microstructure description to the context in which the mesoscale model will be applied. For instance, the number of MSUs can be chosen per the various grain generations that industrial applications may require in order to follow a specific process, while simultaneously requiring only a limited number of variables (five per MSU) to be stored during modeling runs. Such a design opens the possibility of using mechanism-based models of recrystallization even in the context of large FEM simulations. Tested using simple inputs such as constant grain-boundary velocities and nucleation rates, the geometric framework demonstrated its ability to respond in very realistic ways, thus offering great promise for simulations incorporating more physically representative inputs.

VI. NOMENCLATURE

A. *General Rules Regarding Notations*

For any variable, index "i" relates to the MSU to which it belongs. The additional index "j" denotes the MSU with which MSU i is interacting. Indices "e" and "b" refer to grain envelope and intragranular zones properties, respectively. Variation rates with respect to time are denoted with a dot above the variable. For volume variation rates, the superscripts "migr" and "nucl" denote grain-boundary migration and nucleation effects, respectively, and the additional superscript "+" or "-" denotes the sign with which such values contribute to the total variation rate of the considered volume.

Eq. [#] indicates the equation number in which the considered variable is defined.

*Indicates primary variables
**Indicates input variables

List of the main notations for each MSU i

$*v_{ei}$	volume enclosed in the envelope of a grain
$*v_i$	volume of a grain; equals v_{ei} for necklace-only topology
$*V_i$	volume of the MSU
$*\alpha_{xyi}$, α_{xyi}	anisotropy parameters
n_i	volume density of grains (Eq. [2])
D_{eqi}	diameter of a grain of the same volume as that of a grain of MSU i (Eq. [12])
D_i	grain diameter when grains are isotropic; then equals D_{eqi}
D_{xi}, D_{yi}, D_{zi}	principal grain dimensions (Eqs. [13] through [15])

Notations involved in necklace-only interaction probabilities

s_{ei}	surface area of the envelope of an isotropic grain of MSU i (Eq. [6]) surface area of the envelope of an anisotropic grain of MSU i (Eq. [9])
S_{ei}	surface area density of envelopes of MSU i grains in the structure (Eq. [10])
S_{vei}	surface area density of grain boundaries inside MSU i (Eq. [11])
S_{total}	total density of grain envelopes in the structure (Eq. [23])
q_j	probability that a grain boundary is an interface with an MSU j grain (Eq. [23])

Notations involved in necklace-and-intragranular interaction probabilities

X_{bi}	fraction of intragranular areas (Eq. [37])
$**n_{\text{PSN}}$	volume density of PSN sites
$v_{\text{PSN}\,i} v_{\text{PS}Ni}$	volume of intragranular zones per PSN particle (Eq. [39])
n_{bi}	volume density of intragranular zones (Eq. [40])
D_{bi}	diameter of intragranular zones (Eq. [41])
s_{bi}	surface area of intragranular boundaries in a grain of MSU i (Eq. [42])
S_{bi}	surface-area density of intragranular boundaries of grains of MSU i (Eq. [43])
$S_{b\,\text{total}}$	total density of intragranular-zone interfaces in the structure (Eq. [44])
$S_{e\,\text{total}}$	total density of envelope grain boundaries in the structure (Eq. [45])
$S_{ebc\,\text{total}}$	total density of envelope grain boundaries in the structure that can also be intragranular boundaries (Eq. [46])
q_{bei}	fraction of the envelope of a grain of MSU i that is in contact with the intragranular interface of other grains (Eq. [48])
q_{eei}	fraction of the envelope of a grain of MSU i that is in contact with the envelope of other grains (Eq. [49])
q_{eeij}	fraction of the envelope of a grain of MSU i that is in contact with the envelope of grains of MSU j (Eq. [50])
q_{beij}	fraction of the envelope of a grain of MSU i that is in contact with the intragranular interfaces of MSU j (Eq. [51]) fraction of the intragranular interface of a grain of MSU i that is in contact with grain envelopes of MSU j (Eq. [52])

Notations for nucleation

$**\dot{n}_{ei}^{\text{nucl}}$	nucleation rate at the periphery of each grain of MSU i
$**\dot{n}_{bi}^{\text{nucl}}$	nucleation rate at the interface of intragranular zones for each grain of MSU i
$\dot{n}_{i}^{\text{nucl}}$	total nucleation rate for grains of MSU i; equals $\dot{n}_{ei}^{\text{nucl}}$ in the case of necklace-only topology (Eq. [64])
$**v^{\text{nucl}}$	volume of a nucleus

Notation for grain-boundary velocity

$**\dot{u}_{ij}$	velocity of a grain i–grain j boundary

ACKNOWLEDGMENTS

This work was conducted as part of the in-house research activities of the Metals Processing Group of the United States Air Force Research Laboratory's Materials and Manufacturing Directorate. The support and encouragement of the Laboratory management and the Air Force Office of Scientific Research (Dr. J.S. Tiley, program manager) are gratefully acknowledged. One of the authors (JPT) was supported through Air Force Contract No. F33615-03-D-5801.

REFERENCES

1. D. Zhao, C. Cheng, R. Anbajagane, H. Dong, and F.S. Suarez: in *Superalloys 718, 625, 706, and Various Derivatives*, E.A. Loria, ed., TMS, Warrendale, PA, 1997, pp. 163–72.
2. J.T. Yeom, C.S. Lee, J.H. Kim, and N.K. Park: *Mater. Sci. Eng. A*, 2007, vols. A449–A451, pp. 722–26.
3. H.S. Zurob, C.R. Hutchinson, Y. Brechet, and G. Purdy: *Acta Mater*, 2002, vol. 50, pp. 3075–92.
4. G. Shen, S.L. Semiatin, and R. Shivpuri: *Metall. Mater. Trans. A*, 1995, vol. 26A, pp. 1795–1803.
5. J.P. Thomas, E. Bauchet, C. Dumont, and F. Montheillet: in *Superalloys 2004*, K.A. Green, T.M. Pollock, H. Harada, T.E. Howson, R.C. Reed, J.J. Schirra, and S. Walston, eds., TMS, Warrendale, PA, 2004, pp. 959–68.
6. A.D. Rollett, M.J. Luton, and D.J. Srolovitz: *Acta Metall*, 1992, vol. 40, pp. 43–55.
7. R.L. Goetz and V. Seetharaman: *Scripta Mater*, 1998, vol. 38, pp. 405–13.
8. X. Song and M. Rettenmayr: *Comput. Mater. Sci.*, 2007, in press.
9. B. Marty, J.Y. Guedou, P. Gergaud, and J.L. Lebrun: in *Superalloys 718, 625, 706, and Various Derivatives*, E.A. Loria, ed., TMS, Warrendale, PA, 1997, pp. 331–42.
10. C. Sommitsch, V. Wieser, and S. Kleber: *J. Mater. Process. Technol.*, 2002, vols. 125–126, pp. 130–37.
11. P. Poelt, C. Sommitsch, S. Mitsche, and M. Walter: *Mater. Sci. Eng. A*, 2006, vol. A420, pp. 306–14.
12. F. Montheillet: *Proc. 4th Int. Conf. on Recrystallization and Related Phenomena (Rex'99)*, T. Sakai and H.G. Suzuki, eds., Japan Institute of Metals, Sendai, Japan, 1999, pp. 651–58.
13. A. Di Shino and G. Abbruzese: *Proc. 1st Joint Int. Conf. on Recrystallization and Grain Growth*, G. Gottstein and D.A. Molodov, eds., Springer Verlag, Berlin, 2001, pp. 1021–26.
14. S.L. Semiatin, D.S. Weaver, P.N. Fagin, M.G. Glavicic, R.L. Goetz, N.D. Frey, R.C. Kramb, and M.M. Anthony: *Metall. Mater. Trans. A*, 2004, vol. 35A, pp. 679–93.
15. F.J. Humphreys: *Scripta Mater*, 2000, vol. 43, pp. 591–96.
16. R.L. Goetz: *Scripta Mater*, 2005, vol. 52, pp. 851–56.